

Refinement of a theoretical trait space for North American trees via environmental filtering

MICHAEL FELL^{1,2,5} AND KIONA OGLE^{2,3,4}

¹*School of Life Sciences, Arizona State University, P.O. Box 874501, Tempe, Arizona 85287, USA*

²*School of Informatics, Computing & Cyber Systems, Northern Arizona University, P.O. Box 5693, Flagstaff, Arizona 86011, USA*

³*Center for Ecosystem Science & Society, Northern Arizona University, P.O. Box 5620, Flagstaff, Arizona 86011, USA*

⁴*Department of Biological Sciences, Northern Arizona University, P.O. Box 5640, Flagstaff, Arizona 86011, USA*

Abstract. We refer to a theoretical trait space (TTS) as an n -dimensional hypervolume (hypercube) characterizing the range of values and covariations among multiple functional traits, in the absence of explicit filtering mechanisms. We previously constructed a 32-dimensional TTS for North American trees by fitting the Allometrically Constrained Growth and Carbon Allocation (ACGCA) model to USFS Forest Inventory and Analysis (FIA) data. Here, we sampled traits from this TTS, representing different individual “trees,” and subjected these trees to a series of gap dynamics simulations resulting in different annual light levels to explore the impact of environmental filtering (light stress) on the trait space. Variation in light limitation led to non-random mortality and a refinement of the TTS. We investigated potential mechanisms underlying such filtering processes by exploring how traits and the environment relate to mortality rates at the tree, phenotype (a specific set of trait values), and stand (a specific gap scenario) levels. The average light level at the forest floor explained 42% of the stand-level mortality, while phenotype- and tree-level mortality were best explained by six functional traits, especially radiation-use efficiency, maximum tree height, and xylem conducting area to sapwood area ratio (γ_X). These six “mortality” traits and six traits related to the leaf and wood economics spectra were used to construct trait hypercubes represented by trees that died or survived each gap scenario. For trees that survived, the volume of their refined trait space decreased linearly with increasing stand-level mortality (up to ~50% mortality); the location also shifted, as indicated by non-zero distances between the hypercube centroids of surviving trees compared to dead trees and the original TTS. Overall, the patterns were consistent with empirical studies of functional traits, in terms of which traits predict mortality and the direction of the relationships. This work, however, also identified potentially important functional traits that are not commonly measured in empirical studies, such as γ_X and senescence rates of relatively long-lived tissues.

Key words: environmental filtering; functional traits; gap dynamics; hypercube; hypervolume; IBM; North American trees; simulation experiment; trait space; trait spectra.

INTRODUCTION

Quantifying how plant functional traits can determine individual success, and how traits interact with the environment to affect individual performance, is a challenging problem (McMahon et al. 2011, Stahl et al. 2013). Longstanding and recent interest in functional traits encompasses many research areas, including plant competition, community assembly, species coexistence, demographics (Weiher et al. 1999, McGill et al. 2006, Westoby and Wright 2006, Clark et al. 2010, McMahon et al. 2011), biogeography (Violle et al. 2014), global vegetation models (Scheiter et al. 2013, Fyllas et al. 2014, Van Bodegom et al. 2014), and conservation (Devictor et al. 2010). An exciting aspect of functional traits research has been the discovery of correlations among traits representing trade-offs at the global scale. Examples of these include the leaf, wood, and fast-slow economics spectra (Wright et al. 2004, Chave et al. 2009, Reich 2014), and more recently, a global spectrum of plant form and function (Díaz et al. 2016). These spectra are based on correlations found through regression techniques, dimension reduction methods

(e.g., PCA), or other multivariate approaches such as the estimation of convex hulls combined with PCA (Díaz et al. 2016). These approaches have advanced our understanding of the interrelatedness of functional traits, but because they use empirical or statistical models, it is challenging to extend the observed patterns to novel conditions (Pearl and Reed 1920, Webb et al. 2010, Evans et al. 2011).

More robust predictions of plant performance (e.g., growth and survival) in novel environments may be gained by linking trait data to physiological mechanisms (e.g., carbon allocation or plant hydraulics; Savage et al. 2007, Webb et al. 2010, Evans et al. 2011, Scheiter et al. 2013). For example, functional trait distributions are influenced by both environmental and biotic filters that lead to non-random mortality, favoring individuals that can survive in a given environment (Van der Valk 1981, Woodward and Diament 1991, Weiher and Keddy 1999, Webb et al. 2010). The ways in which individuals respond to these filters are limited by inherent mass balance (e.g., the amount of a resource allocated to particular functions cannot exceed what is available) and engineering constraints (e.g., plant architectures have to be mechanically feasible; Scheiter et al. 2013). Environmental filters tend to limit the range of trait distributions in a given environment; these filters relate to limiting factors such as resources, temperature, or soil characteristics (Van der Valk 1981,

Manuscript received 8 December 2017; accepted 2 January 2018.
Corresponding Editor: Peter B. Adler.

⁵E-mail: michael.fell@nau.edu

Woodward and Diament 1991, Weiher and Keddy 1999, Webb et al. 2010), and variation in these factors tends to select for plants that remain above their zero-net-growth isoclines (Tilman 1985). Biotic filters such as interspecific competition can limit the similarity of the remaining species traits in a community (MacArthur and Levins 1967, Stubbs and Wilson 2004, Cornwell and Ackerly 2009). Thus, both environmental and biotic filters can lead to non-random mortality, and one way to investigate how filtering influences the trait space is to identify the traits that are the best predictors of mortality in different environments.

This study focuses on tree functional traits affecting carbon acquisition, allocation, and utilization, all of which are key to understanding tree growth, mortality, and fitness (Poorter 1999, Poorter and Bongers 2006, Wright et al. 2010). For many boreal and temperate forests, canopy gap dynamics can produce widely varying environmental conditions, potentially acting as an important filtering process leading to non-random mortality (McCarthy 2001). For example, forest gap formation and closure are important in determining community dynamics (Runkle 1985, Runkle and Yetter 1987). Tree success can depend on gap dynamics, which directly impacts light availability and hence, carbon uptake; gap dynamics include how often gaps form, how long the gap remains open, and how long it takes for the forest canopy to close (Runkle 1985, Valverde and Silvertown 1997, McCarthy 2001, Ogle and Pacala 2009). Thus, we expect canopy gap dynamics to impact the multidimensional trait space of trees through non-random mortality. However, studying the impact of gap dynamics on the trait space of trees growing in the field is challenging for at least two reasons. The long time scales over which gap dynamics operate and the long life span of trees makes it difficult to follow such processes in the field. Secondly, it is possible that key functional traits related to growth and mortality under various gap dynamics may not be traits that are easily measured in the field.

The aforementioned issues point to the utility of using simulation models. Thus, we draw upon the semi-mechanistic Allometrically Constrained Growth and Carbon Allocation (ACGCA) model developed by Ogle and Pacala (2009), which predicts tree growth, carbon allocation, and survival status at annual time-steps, given average, annual light levels above the forest canopy. In particular, ACGCA encapsulates much of our understanding of tree growth processes, including known tree allometries (well-studied empirical relationships), along with physiological and morphological traits (representing carbon-mass-balance mechanisms), which control carbon allocation from a transient (fast) pool to a storage (slow) pool and structural compartments within an individual tree (Ogle and Pacala 2009). Tree death occurs if the non-structural carbohydrate (slow and fast) pools are depleted (Ogle and Pacala 2009). The ACGCA model offers a tool for conducting simulation experiments for which corresponding field experiments cannot be implemented at a comparable scale; i.e., we must follow a large number of trees over a sufficiently long time period to observe a sufficient number of mortality events. The semi-mechanistic underpinnings of the ACGCA model and the inclusion of traits that are rarely measured in the field (e.g., xylem conducting area, senescence rates, construction costs, and labile carbon storage capacity) provides additional advantages of simulation experiments over field campaigns.

We integrated the ACGCA model with a simple gap dynamics simulator to investigate if an individual tree, defined by a specific set of functional trait values, is capable of surviving a particular gap dynamics scenario. We imposed a wide range of realistic gap scenarios leading to varying levels of environmental stress (Ogle and Pacala 2009), to investigate the relationship between selective mortality due to environmental filtering (light stress) and tree traits (ACGCA parameters). Through repeated simulation, we used the gap dynamics scenarios to explore how the multidimensional trait space changes with increasing stress (filtering), and to learn which traits experience the greatest filtering and/or are the best predictors of mortality.

In previous work, we used the ACGCA model to estimate the theoretical trait space (TTS) for North American trees (see Table 1 for a full list of traits; Fell et al. 2018). This was done by fitting the ACGCA model to USFS Forest Inventory and Analysis (FIA) data while restricting parameter values to realistic ranges through the use of semi-informative, literature-based priors. The TTS represents the trait space that is consistent with *living* trees in the FIA data, regardless of species identity or site factors. In this study, our objective was to assess how this TTS may be refined when applying the ACGCA model to a range of gap dynamics simulations that lead to some level of mortality (i.e., not all simulated trees survive). In doing so, we address the following questions: (1) How do environmental factors, such as time between gaps and average light level, relate to mortality rates at different scales (stand, phenotype, tree)? (2) Which functional traits are the best predictors of phenotype- and tree-level mortality? (3) To what degree does environmental filtering associated with the gap scenarios lead to a refinement of the trait space relative to the original TTS? For the latter question, we explore how the trait space differs between trees that survived vs. those that died, or between surviving and dead trees vs. the original TTS.

METHODS

Theoretical trait space

The ACGCA model involves 32 parameters (inputs) representing physiological, morphological, and allometric traits (see Table 1 for ACGCA parameter definitions, and Appendix S1: Table S1 for TTS trait ranges). We used parameter values (trait values) representative of the theoretical trait space (TTS) of North American trees based on previous work (Fell et al. 2018) that simulated 33,000 parameter sets, each representing a vector of 32 parameters (traits), from the TTS. These parameter sets were found by fitting the ACGCA model to U.S. Forest Service Forest Inventory and Analysis (FIA) data, including remeasurements of tree heights and diameters, and their estimated annual rates of change (data *available online*).⁶ The model was fit to the FIA data via a simple Bayesian framework that employed a custom Metropolis-Hastings (MH) algorithm to sample from the posterior of the parameters, which was evaluated to explore the joint and marginal parameter spaces for each trait in the ACGCA model. The likelihood

⁶ <http://www.fia.fs.fed.us/>

TABLE 1. Descriptions of the 32 parameters (θ_k) in the ACGCA model that represent tree functional traits, including units of the parameters.

Symbol	Unit	Description
H_{\max}	m	maximum tree height
φ_H		slope at H vs. r curve at $r = 0$ m
η		relative height at which trunk transitions from paraboloid to cone
SW_{\max}	m	maximum sapwood width
λ_S		proportionality between B_T and B_O for sapwood
λ_H		proportionality between B_T and B_O for heartwood
ρ	g dm/m ³	wood density
f_1		fine root area to leaf area ratio
f_2		leaf area to xylem conducting area ratio
γ_C	g gluc/m ³	maximum storage capacity of living sapwood cells
γ_W	m ³ /g dm	(inverse) density of sapwood structural tissue
γ_X		xylem conducting area to sapwood area ratio
C_{gL}	g gluc/g dm	construction costs of producing leaves
C_{gR}	g gluc/g dm	construction costs of producing fine roots
C_{gW}	g gluc/g dm	construction costs of producing sapwood
δ_L	g gluc/g dm	labile carbon storage capacity of leaves
δ_R	g gluc/g dm	labile carbon storage capacity of fine roots
S_L	yr ⁻¹	senescence rate of leaves
SLA	m ² /g dm	specific leaf area
S_R	yr ⁻¹	senescence rate of fine roots
S_O	yr ⁻¹	senescence rate of coarse roots and branches
r_R	m	average fine root radius
ρ_R	g dm/m ³	tissue density of fine roots
R_{mL}	g gluc g-dm ⁻¹ ·yr ⁻¹	maintenance respiration rate of leaves
R_{mS}	g gluc g-dm ⁻¹ ·yr ⁻¹	maintenance respiration rate of sapwood
R_{mR}	g gluc g-dm ⁻¹ ·yr ⁻¹	maintenance respiration rate of fine roots
η_B		relative height at which trunk transitions from neiloid to paraboloid
k		crown light extinction coefficient
ε	g gluc/MJ	radiation-use efficiency
m		maximum relative crown depth
α		Crown curvature parameter
R_0	m	maximum potential crown radius of a tree with dbh of 0 m (i.e., for a tree that is exactly 1.37 m tall)
R_{40}	m	maximum potential crown radius of a tree with dbh of 0.4 m (40 cm)

Notes: Empty cells indicate unitless parameters. Abbreviations are dm, dry mass; gluc, glucose; dbh, diameter at breast height. Table follows from Ogle and Pacala (2009).

of the modeled (ACGCA) outputs, annual heights, diameters, and rates of change, was evaluated against a four-dimensional histogram representing realistic tree growth based on 1.27 million FIA remeasurements of height, radius, change in height, and change in radius for living, healthy trees (i.e., data for dead trees or trees associated with no growth or negative growth were eliminated). The ACGCA model parameters were further constrained by informative prior distributions based on the TreeTraits literature database (Kattge et al. 2011, Ogle et al. 2013, 2014) and/or values used to develop and test the ACGCA model (Ogle and Pacala 2009), as described in Fell et al. (2018). The final output from this analysis (posterior samples of the parameters [or traits]) can be thought of as representing an unfiltered trait space, or the TTS, that simultaneously agrees with FIA data, the semi-informative priors, and the ACGCA model structure.

Gap dynamics simulations

The overarching goal of the gap dynamics simulations was to impose environmental (light) stress on the aforementioned

unfiltered trait space (the TTS). Though it could be argued that gap dynamics simulations really impose a biotic stress due to competition for light by surrounding trees, as opposed to a strictly abiotic (i.e., environmental) stress (Kraft et al. 2015), the sole effect of the gap formation and closure process in our simulations is to increase light availability during the (short) open gap phase, and greatly reduce light availability during the (relatively long) closed canopy phase. Regardless of which perspective is employed (abiotic vs. biotic stress), the gap dynamics scenarios are constructed to explore how varying stress conditions may refine the TTS by potentially eliminating sub-regions of the trait space, associated with trees (or sets of trait values) that die during the simulation. Our gap scenarios are based on those described in Ogle and Pacala (2009); only details relevant to our objectives and questions are provided here. The mortality output and TTS data are available via Dryad (see *Data Availability*).

Gap simulations were conducted with three repeated phases: open gap, gap closure, and closed canopy. Following Ogle and Pacala (2009), three levels were used for the open gap phase (gt = 4, 6, and 8 yr), five for the closure phase

(ct = 5, 10, 15, 25, and 45 yr), and five for the time between gaps (tbg = 20, 35, 50, 100, and 200 yr). Some combinations were removed due to inconsistencies (e.g., a time between gaps of 20 yr and a closure phase of 45 yr are inconsistent), resulting in 62 unique simulation scenarios. Each scenario was run for a 200-yr period, and the average light at the forest floor was calculated for this period based on supplemental material in Ogle and Pacala (2009), using a standard Beer-Lambert light-extinction model, combined with modeled variation in forest canopy leaf area index (LAI_F) as gaps form and close. Average light level at the forest floor (PAR_{avg}) was found to be closely related to tbg and stand/scenario-level mortality (see *Results*), and thus was used as a continuous variable representative of the level of environmental stress in a subset of regression analyses described below.

The gap scenario simulations were kept simple by employing an empirical model that described the LAI_F of the surrounding forest canopy, rather than modeling individual trees in the surrounding forest. The ACGCA model, however, was used to model growth and survival of the target tree defined by a particular set of parameters (traits), under each gap scenario. The forest was prescribed a canopy height (H_F) and LAI_F, both of which were zero during the gap phase and both increase linearly during the closure phase, until reaching their maximum values during the closed phase (Ogle and Pacala 2009). The forest canopy affects the modeled (target) tree through its effect on annual photosynthetically active radiation (APAR) according to the Beer-Lambert equation (Ogle and Pacala 2009). The light environment experienced by the target tree is determined by its crown height (H) relative to H_F, yielding three scenarios: (1) the tree is not limited by light (H > H_F), (2) its crown is partially exposed to full sunlight (H_η < H_F < H, where H_η is the height to the base of the target tree's crown), or (3) the tree can be completely overtopped by the surrounding forest (H_F > H; Ogle and Pacala 2009).

Output from the gap dynamics simulations was used to determine if a given parameter set led to a target tree that survived or died over the 200-yr period, for each of the 62 gap scenarios. This yielded 2,046,000 (33,000 parameter sets × 62 gap scenarios) binary values, where 0 indicated a tree that survived the 200-yr simulation, and 1 indicated death during the simulation. These binary outputs were summarized to quantify three types of mortality (Table 2). For the first type of mortality, the individual binary values are representative of tree-level mortality (m_{g,p}) for gap scenario g (g = 1, 2, ..., 62) and parameter (trait) set p (p = 1, 2, ..., 33,000), which were used to evaluate how environmental factors vs. functional traits explain m_{g,p} (addressing question 1 and 2). Two additional indices of mortality, stand-level (denoted by m_g^S) and phenotype-level (denoted by m_p^θ), summarize mortality rates for each gap scenario (m_g^S, for g = 1, 2, ..., 62) or for an individual set of parameters (m_p^θ, for p = 1, 2, ..., 33,000), respectively (Table 2).

Mortality associated with each gap scenario (m_g^S) can be thought of as an index of stand-level mortality since each set of traits was subjected to a fixed environment within each gap scenario. In particular, for each gap scenario g

TABLE 2. Methods of calculating mortality are shown relative to the simulation design.

	θ (unique traits vector)				Stand-level simulation
	θ ₁	θ ₂	...	θ _{33,000}	
Gap scenarios					
1	1	0	...	1	m ₁ ^S
2	0	1	...	0	m ₂ ^S
3	1	1	...	0	m ₃ ^S
⋮	⋮	⋮	⋮	⋮	⋮
⋮	⋮	⋮	⋮	⋮	⋮
⋮	⋮	⋮	⋮	⋮	⋮
61	1	1	...	0	⋮
62	0	1	...	1	m ₆₂ ^S
Phenotype level	m ₁ ^θ	m ₂ ^θ	...	m _{33,000} ^θ	

Notes: Each binary entry in the table represents a single instance of a given vector of unique values for the 32 traits (θ) listed in Table 1, with each vector being subjected to a given gap dynamics scenario (62 total scenarios); the binary entries indicate tree-level mortality (m_{g,p}; 1 = died, 0 = survived). The gap scenarios can be thought of as representing different environments, with each denoting an environment for a particular forest stand. Thus, stand-level mortality (m_g^S) is found by averaging across all 33,000 columns (across all trait vectors) for each row to obtain the proportion of trees that died in each gap scenario (stand). Each unique vector of θ, representing a particular “phenotype,” is subjected to 62 gap scenarios. Thus, phenotype-level mortality (m_p^θ) is found by averaging across all 62 rows within each column, giving the proportion of trees that died across all 62 gap scenarios, for each unique combination of θ values.

$$m_g^S = \frac{\sum_{p=1}^{33,000} m_{g,p}}{33,000} \tag{1}$$

Thus, there are 62 m_g^S values of stand-level mortality, one for each gap scenario; these mortality values were analyzed to evaluate how environmental factors (e.g., time between gaps or PAR_{avg}) relate to stand-level mortality (question 1).

Phenotype-level mortality (m_p^θ) was calculated for each parameter set p drawn from the original (unfiltered) TTS (Fell et al. 2018). Each unique parameter set can be viewed as a phenotype since it represents a specific combination of functional trait values within the TTS. Phenotype-level mortality was calculated as

$$m_p^\theta = \frac{\sum_{g=1}^{62} m_{g,p}}{62} \tag{2}$$

These mortality values were analyzed to evaluate if, and which, functional traits can explain m_p^θ (question 2). Both m^S and m^θ describe the proportion of trees that died for each gap scenario and phenotype (parameter set), respectively (see Table 2).

Statistical analyses

Mortality regressions.—We conducted stepwise regression analyses to evaluate the factors underlying tree-, stand-, and phenotype-level mortality (to address questions 1 and 2). In all cases, the Bayesian information criterion (BIC) was used for the model selection criterion because it has a greater penalty term for each added variable and it tends to select more

parsimonious models (Gelman et al. 2014). All stepwise regressions used forward and backward selection.

We evaluated how well the environment and functional traits explain tree-level mortality (questions 1 and 2), $m_{g,p}$ (given by 0 [survived] or 1 [died]), by conducting three logistic, stepwise regression analyses: (1) light + trait model, (2) trait-only model, and (3) light-only model. Each model was fit to one-half of the $m_{g,p}$ values ($n = 1,023,000$), chosen randomly from the full data set. The remaining 50% of the $m_{g,p}$ values (not selected above) were used as a test data set to assess the extent to which $m_{g,p}$ could be correctly predicted by each model. The light + trait model included each of the 32 functional traits associated with each p and the average light level (PAR_{avg}) for each gap scenario g as potential predictors of $m_{g,p}$. Two-way interactions between PAR_{avg} and each of the 32 traits were included in the full model to account for differing effects of the traits depending on light level. The trait-only model included only the functional trait values associated with each p , and the light-only model included PAR_{avg} associated with each g as the sole explanatory variable.

The relationship of stand-level mortality (m_g^S) to environmental factors (question 1) was addressed by regressing the 62 m_g^S values on each of the gap dynamics variables (gt , ct , and tbg) associated with each scenario g . We treated gt , ct , and tbg as categorical factors in the regressions. Another simple linear regression was carried out by regressing m_g^S on the PAR_{avg} of each scenario g . These regression models allowed assessment of which aspect of the gap dynamics process (environment) best explained mortality at the stand level. This also allowed us to confirm that PAR_{avg} was an effective composite variable representing the environment in each simulation.

To evaluate the factors affecting phenotype-level mortality (m_p^0 ; question 2), we conducted a stepwise regression where each of the 33,000 m_p^0 values were regressed on the 32 trait values associated with parameter set p . Two regressions were conducted; one with only main effects (main-effects-only model) and another including main effects and all two-way interactions among each of the 32 traits (interaction model). Since m_p^0 averages across all gap scenarios, an index of light availability is irrelevant to understanding variation in m_p^0 . The relative importance of each parameter in the main effects only model was determined using the `relaimpo` package in R (Grömping 2006), which computes the proportion of variation explained by each trait (independent variable) relative to the total variation explained (R^2) by the model. This was only done for the main effects-only model; the complexity of the interaction model and the sample size led to computational challenges when trying to calculate the relative importance (the computer's memory was exceeded). The results from an analysis using partial R^2 values to identify the most important predictors (trait) of mortality are given in Appendix S1: Fig. S1 for both the main effects-only and the interaction model.

Hypercube trait space analysis.—We evaluated how the trait space changed with the filtering introduced by the gap scenarios (question 3). As a simple qualitative analysis, plots of kernel density estimates for each trait were constructed for each gap scenario for surviving and dead trees (32 traits \times 62 scenarios \times 2 types [dead or living]) to visualize the separation

in trait space between surviving and dead trees for individual traits. A more rigorous evaluation of the emergent trait spaces was achieved by using the hypercube package in R (Blonder et al. 2014), which allowed us to quantitatively assess how the multi-dimensional trait space (i.e., hypervolume) shifts as a result of environmental stress. The hypercube package characterizes high-dimensional spaces, and was used to estimate hypercube volumes and centroid distances between two hypercubes. We constructed hypercubes for the trees that survived and for those that died during each of the 62 gap scenarios. The number of parameter sets (trees) differed among the surviving and dead groups due to differing mortality rates in each gap scenario. For instance, while 33,000 trees were simulated in each scenario, one-half of the trees may have died in one scenario, while only a little over 3,000 died in another, leading to different sample sizes for surviving and dead trees. Thus, to construct hypercubes for each stand (gap scenario) and each group of trees, 3,000 parameter sets were randomly sampled from each group, without replacement, to avoid potential problems due to differences in sample sizes.

To ensure that the above subsampling did not bias our results, the analysis was repeated 100 times to assess the effect of subsampling. Furthermore, we also randomly sampled from the (unfiltered) TTS to construct a data structure similar to each gap scenario; for example, if N_g^D trees died and N_g^S trees survived gap scenario g , we randomly drew, without replacement, two groups of parameters sets from the TTS of size N_g^D and N_g^S . These samples were then further subsampled by randomly selecting 3,000 parameter sets from each group, which were subsequently used to construct hypercubes representative of the TTS and to evaluate the potential effect of differential sample size on the hypercube results.

One limitation of the hypercube method is that the number of dimensions cannot exceed the natural log of the sample size (Blonder et al. 2014). In the case of our model output, this allowed a maximum of eight dimensions (i.e., $\log_e(3,000) = 8.01$), though we only used six. For these analyses, we used a quantile of 0.05 (95% included) and a bandwidth of 0.4 (the lowest value that did not cause errors); the bandwidth affects the smoothness of the fit to the data (see Blonder et al. 2014, for additional details). With this in mind, the six traits with the greatest relative importance (accounting for over 90% of the R^2) in explaining m_p^0 were included (i.e., H_{max} , ϵ , γ_X , S_O , R_{mL} , and R_0 ; see Fig. 1, and Table 1 for a description of the traits); hereafter referred to as the “mortality traits.” We also constructed hypercubes based on six traits related to the leaf economics spectrum (LES) and wood economics spectrum (WES; i.e., SLA , ϵ , R_{mL} , S_L , γ_X , and ρ); hereafter referred to as the “leaf/wood traits.” For each group of traits (mortality traits and leaf/wood traits), we used the aforementioned subsampling procedure to construct hypercubes for the surviving and dead trees for each gap scenario, as well as for the original TTS, which is independent of gap scenario.

Using the aforementioned (three) constructed hypercubes, the traits of surviving and dead trees were compared to each other as well as to the TTS, allowing us to assess if light stress results in a refinement of the trait space. In particular, comparisons of the trait spaces represented were made by calculating the centroid distances and difference in volumes between pairs of hypercubes. Centroid distances and volume

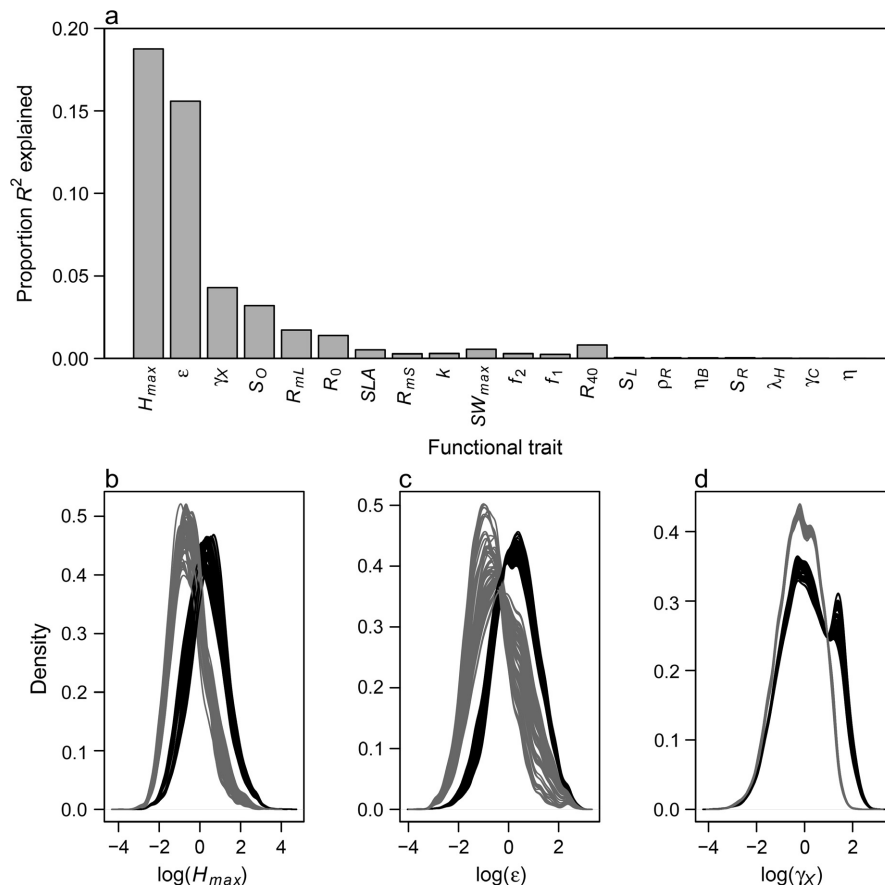


FIG. 1. Summary of traits (parameters) predictive of phenotype-level mortality (m_p^0). (a) Variables on the x -axis are the traits (see Table 1 for definitions) included in a stepwise regression for m_p^0 that only considered the main effects of each trait. The bars indicate the relative importance of each trait based on its R^2 (coefficient of determination) contribution, as determined with the lmg method in R, which averages over all possible orderings of variables in the model. The sum of the R^2 proportions gives the overall R^2 of 0.48. For the top three traits in panel a, kernel density estimates are shown for normalized (b) log maximum tree height (H_{max}), (c) log radiation-use efficiency (ϵ), and (d) log proportion of xylem conducting area (γ_X). In panels b–d, gray lines denote trees that died during the gap simulations and black lines denote trees that survived; 62 lines are overlaid for each group (dead and live), one for each gap scenario.

differences were found between the TTS hypercube and the surviving and dead hypercubes (TS is TTS vs. surviving hypercubes, TD is TTS vs. dead hypercubes), and between the surviving and dead hypercubes (SD is surviving vs. dead hypercubes), for each of the 62 gap dynamics scenarios. When calculating volume differences, surviving and dead hypercube volumes were subtracted from the TTS hypercube volume (TTS served as the reference). When comparing the surviving and dead hypercubes, the surviving hypercube served as the reference. For hypercubes representing both mortality traits and leaf/wood traits, linear regressions were used to evaluate how centroid distances and volume differences varied with stand-level mortality (m_g^S). This resulted in 12 regressions; three (TS, TD, SD) for centroid differences, three (TS, TD, SD) for volume differences, with each repeated for the two set of traits (mortality and leaf/wood).

RESULTS

Mortality regressions

Tree-level mortality.—The logistic regressions for tree-level mortality ($m_{g,p}$) show that the light + trait model correctly

predicted a tree's live/dead status in 82% of the validation cases (test sample), while the trait-only model had comparable (80% correct) results. The light-only model was notably inferior (42% correct; Fig. 2). The light-only model performed poorly because it tended to predict that nearly all trees died such that it correctly classified 95% of the dead trees, but misclassified 90% of the surviving trees (Fig. 2). By comparison, the traits-only and traits + light models predicted dead trees correctly in 67% and 72% of the test samples, respectively, and classified surviving trees correctly in 87% and 88% of the test samples, respectively.

Based on the stepwise regression models involving traits, the specific traits that had the greatest effect sizes (all significant at $P < 0.01$) on $m_{g,p}$ were, in order of decreasing importance, ϵ (negative effect), H_{max} (negative), γ_X (negative), S_O (positive), R_{mL} (positive), and R_0 (negative) for the traits-only model (see Table 1 for definitions of the traits and Appendix S1: Table S2 for effect sizes). For the light + traits model, the traits or predictors with the largest effect sizes were ϵ (negative), H_{max} (negative), γ_X (negative), PAR_{avg} (negative), S_O (positive), and R_{mL} (positive) (see Appendix S1: Table S3); some of these traits overlap with the traits-only model, but clearly light level is also an important predictor of

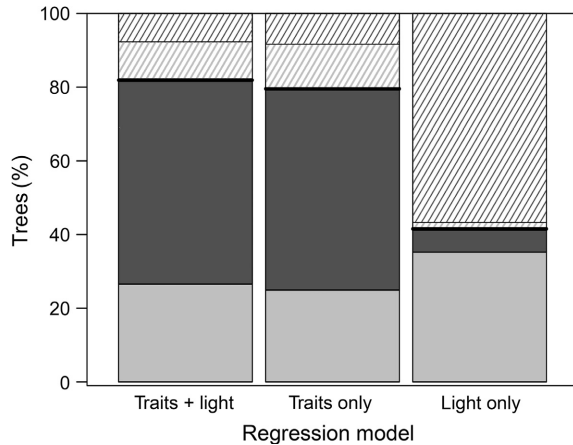


FIG. 2. Percentage of trees correctly or incorrectly classified ($n = 1,023,000$) as dead or surviving based on applying each of the three stepwise, logistic regression models of tree-level mortality ($m_{g,p}$) to a hold-out (test) data set. Within each bar, the color (solid or striped) indicates the true status of a tree in the hold-out data set, with dark gray indicating surviving trees and light gray indicating dead trees. The two boxes with solid shading, below each thick horizontal line, indicate hold-out data that were correctly predicted by the regression model, whereas striped boxes above the thick line indicate incorrect predictions. The traits-only model included the main effects of all 32 Allometrically Constrained Growth and Carbon Allocation (ACGCA) traits, but excluded light; the traits + light model included the 32 traits, the average light level (PAR_{avg}), and all two-way interactions between PAR_{avg} and each trait; the light-only model only included PAR_{avg} (no traits). Overall, the light-only model was best at identifying trees that died, but it did very poorly at identifying trees that survived. The models that included the traits produced similar results and successfully identified living trees far better than when only PAR_{avg} was considered.

tree-level mortality. See Appendix S1: Tables S2–S4 for a more detailed summary of the results (effects) from the three logistic regression models.

Stand-level mortality.—Of the three gap phase variables, time between gaps (tbg) was the best predictor ($P < 0.05$) of stand-level mortality (m_g^S), and the model that only included this factor (five levels) yielded $R^2 = 0.74$ (Appendix S1: Table S5 and Fig. 3a). Mortality increased with increasing tbg in a non-linear fashion such that m_g was less sensitive to tbg at higher values. The regressions modeling m_g^S as a function of either gap period (gt) or gap closure time (ct) yielded worse fits ($R^2 = 0.002$ and 0.052 , respectively). Finally, when m_g^S was regressed on the average light level at the forest floor (PAR_{avg}) over the 200-yr simulation, PAR_{avg} was a significant predictor of m_g^S ($P < 0.05$, $R^2 = 0.85$, Fig. 3b).

Phenotype-level mortality.—The step-wise regression for phenotype-level mortality (m_p^0) that only involved main effects of tree traits converged to a model involving 20 of the original 32 traits ($R^2 = 0.48$; Appendix S1: Table S6). The model that included main effects and two-way interactions included 72 effects, representing 22 main effects and 50 interaction terms ($R^2 = 0.62$; Appendix S1: Table S7), indicating that inclusion of trait interactions improves our ability to predict mortality. Based on the main effects only model, the six traits with the greatest effect sizes were ϵ (negative), H_{max} (negative), γ_X (negative), S_O (negative), R_{mL}

(positive), and R_0 (negative) (Appendix S1: Table S6), and these traits accounted for over 93% the overall R^2 (Fig. 1a). Though the relative importance (R^2 contribution) of each term could not be calculated for the model including interactions, of the main effects, these same six traits emerged among the top nine with the greatest effect sizes, and they maintained the same relationships to mortality (negative or positive; see Appendix S1: Table S7).

The multi-dimensional trait space

A general shift was seen in the marginal distributions (i.e., kernel density estimates) for parameters (traits) with larger effect sizes in the mortality regressions, as seen by a separation between the distributions of traits associated with trees that survived a simulation vs. those that died (Fig. 1b–d). However, such a separation is not apparent for traits that were non-significant predictors of mortality.

Centroid differences.—The hypercube analysis for the top six traits (ϵ , H_{max} , γ_X , S_O , R_{mL} , and R_0) identified as the most significant predictors of tree- and phenotype-level mortality clearly indicated shifts in the trait spaces for the surviving and dead trees in the context of the gap dynamics simulations. Centroid differences between surviving trees vs. the TTS (TS) had a significant positive relationship with stand-level mortality (m_g^S ; $R^2 = 0.96$, $P < 0.01$), indicating greater divergence between the functional traits of surviving trees relative to the TTS as mortality increases. Distances ranged from 0.18 to 0.65 across the 62 gap scenarios (distances are unitless because trait values were normalized relative to their posterior standard deviations, Fig. 4a). This range exceeds the mean and maximum centroid distances of 0.14 and 0.18, respectively, found by randomly sampling the TTS (Fig. 4a). Distances between centroids for trees that died vs. the TTS (TD) had a significant negative relationship with m_g^S ($R^2 = 0.95$, $P < 0.01$) indicating that the trait space of dead trees and the TTS are most dissimilar under low mortality rates, with minimum and maximum distances of 0.54 and 1.02, respectively (Fig. 4b). Finally, distances between centroids for surviving vs. dead (SD) trees had a significant negative relationship with m_g^S ($R^2 = 0.99$, $P < 0.01$), with a range from 0.15 to 0.79 (Fig. 4c). That is, as m_g^S increases, the centroids of the surviving and dead trees converge to similar values (Fig. 4c). These results were essentially the same when the analysis was repeated for six leaf/wood traits related to the LES and WES (Appendix S1: Fig. S2a–c), with comparable R^2 values of 0.95, 0.94, and 0.99 for TS, TD, and SD, respectively.

Volume differences.—Differences between hypercube volumes for both groups of traits (mortality and leaf/wood traits) followed the same patterns as the centroid distances, with all models being statistically significant ($P < 0.01$). Volume differences spanned a minimum and maximum of ~ 0 to 51.06, 24.01 to 98.20, and -14.65 to 81.64 for the TS, TD, and SD comparisons of the mortality traits, respectively; these differences demonstrate a restriction (shrinking) of the trait space of both surviving and dead trees as m_g^S increases up to 50%. The volume differences between the three hypercubes (TS, TD, and SD) exceeded the null model found by

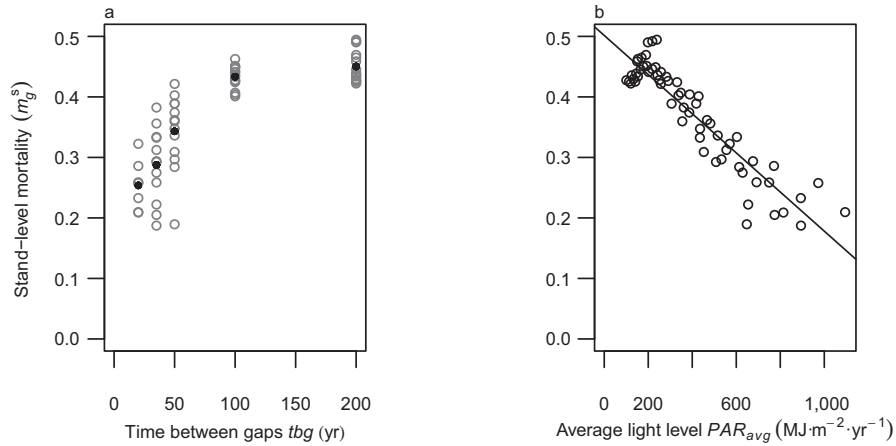


FIG. 3. Linear models of stand-level mortality (m_g^S) as explained by (a) time between gaps (tbg) treated as a factor and (b) mean annual light level at the forest floor (PAR_{avg} ; continuous covariate). In panel a, black symbols are the average mortality across all gt (gap time) and ct (closure time) levels within each tbg level; open circles are the mortality values for each combination of gt and ct . (a) Among the three gap phase variables (tbg , gt , ct), tbg was the best predictor of m_g^S ($P < 0.05$, $R^2 = 0.74$) and (b) PAR_{avg} was the overall best predictor of m_g^S ($P < 0.05$, $R^2 = 0.85$).

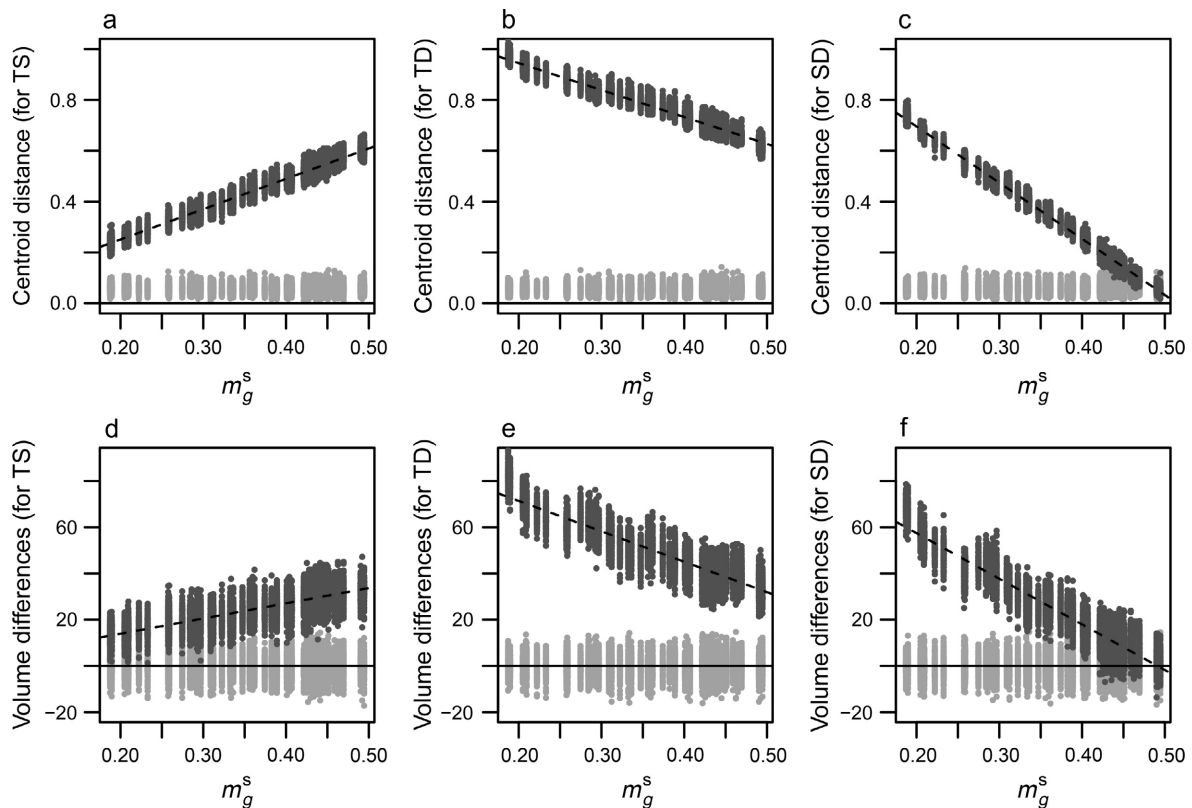


FIG. 4. Hypercube centroid distances and volume differences based on six-dimensional hypercubes constructed from the “mortality” traits (H_{max} , ϵ , γ_X , S_O , R_{mL} , and R_0 ; see Table 1 for definitions of the traits), as a function of stand-level mortality (m_g^S). TS compares hypercubes representing the theoretical trait space (TTS) vs. surviving trees; TD compares the TTS vs. trees that died; SD compares surviving vs. dead trees. In particular, centroid differences are shown for (a) TS, (b) TD, and (c) SD, and volume differences for (d) TS (i.e., TTS volume – surviving volume), (e) TD (TTS – dead), and (f) SD (surviving – dead). Dark gray points show estimates for each gap scenario, with the range of values obtained by randomly sampling 3,000 points from the TTS, surviving, and dead trait spaces, for each of the 62 gap dynamics scenarios. Dashed black lines show the linear best fit of the distances or volume differences vs. m_g^S (stand-level mortality). Light gray points show results from performing the same analysis for data sampled at random from the TTS to ensure the resultant patterns were not an artifact of the analysis structure.

randomly sampling the TTS, which yielded mean and maximum volume differences of 0.006 and 0.021, respectively. Though the trends in volume differences were in the same direction as those for centroid distances, mortality (m_g^S) explained less of the variation in the volume differences; $R^2 = 0.47, 0.78,$ and 0.84 for TS, TD, and SD, respectively (Fig. 4d–f). Volume differences between surviving and dead trees are greatest under lower stand-level mortality (m_g^S), with dead trees associated with more restricted trait spaces, but these differences disappear as m_g^S approaches 50% (Fig. 4f). These results for the hypercube volumes are essentially the same when repeated for the leaf/wood traits; regressions of the volume differences vs. m_g^S gave $R^2 = 0.59, 0.82,$ and 0.90 for TS, TD, and SD, respectively (Appendix S1: Fig. S2d–f).

DISCUSSION

Mortality and functional traits

We first discuss our results in the context of our first research question focusing on how stand-level mortality is related to environmental factors (average light at the forest floor and gap simulation variables). Next, we discuss results for both tree- and phenotype-level mortality simultaneously, in the context of our first and second questions, addressing how environment (light) vs. functional traits explain tree-level mortality, and we identify which functional traits (parameters) predict phenotype-level mortality (question 2). Then, we discuss how environmental filtering (light stress) refined the trait space relative to the TTS, and how the trait spaces differed among surviving and dead trees (question 3). Finally, we follow this with an evaluation of how our results compare to empirical trait-mortality patterns reported in the literature.

Stand-level mortality.—Regarding the influence of environmental factors on stand-level mortality (question 1), we found that the average light level at the forest floor (PAR_{avg}) was an excellent predictor of stand-level mortality (m_g^S ; Fig. 3b). While time between gaps (tbg) was also a good predictor of stand-level mortality (Fig. 3a), with longer times leading to higher mortality rates, other indices of the gap phase, such as the length of the forest gap (gt) during which a tree could experience high light or the time it takes for the forest canopy to close after a gap has formed (ct), offered little insight into stand-level mortality. PAR_{avg} is ultimately a function of the three gap phase variables (tbg, gt, and ct), and thus, it is not surprising that PAR_{avg} was the best predictor of stand-level mortality. For example, of the three gap phase variables, tbg most strongly influenced PAR_{avg} (Appendix S1: Fig. S3a–c), especially for large tbg, in which case the gap length (gt) and closure time (ct) were less important. In the most extreme case, where tbg was equal to the simulation length (200 yr), a gap was created at the beginning of the simulation, followed by canopy closure and an extended closed canopy phase, leading to comparatively low PAR_{avg} and high mortality.

We note that, in our simulation study, functional traits were irrelevant for understanding stand-level mortality since we did not simulate communities of trees, but simply

evaluated the proportion of individually simulated trees that died during each gap scenario (a “stand”). For modeling approaches that consider an entire community of trees competing explicitly for resources, such as the JABOWA (Botkin et al. 1972, Bugmann 2001), SORTIE (Pacala et al. 1993, 1996), or Ecosystem Demography (Moorcroft et al. 2001) models, one could compute community-weighted functional traits to determine the importance of traits for predicting stand-level mortality.

Tree- and phenotype-level mortality.—With respect to how the environment (question 1) and functional traits (question 2) explain mortality, we found that simulated tree-level mortality ($m_{g,p}$) was better explained by functional traits rather than by PAR_{avg} (environment; Fig. 3). This may not be surprising given that PAR_{avg} served as the only environmental predictor, while a total of 32 functional traits were considered. PAR_{avg} alone successfully predicted death for trees that actually died, but it also predicted that most surviving trees would have died during the 200-yr simulation. In cases where simulated trees died, death was ultimately due to carbon starvation resulting from low light. However, the actual light level experienced by the tree, which was not tracked as such data would be difficult to obtain for real trees, over the simulation period is mediated by the tree’s crown height relative to the forest canopy. Due to this, PAR_{avg} , the quantity considered here, alone cannot discriminate between trees that could succeed when overtopped (shade tolerators) vs. trees that can grow above the forest canopy (shade avoiders; e.g., Givnish 1988, Falster and Westoby 2005). Hence, PAR_{avg} appears only informative for predicting mortality if key functional traits are also considered.

Regarding mortality rates of specific phenotypes, we found that functional traits in the TTS reasonably explained variation in phenotype-level mortality (m_p^0). In particular, 48% of the variation was explained by the independent effects of 20 traits, and 62% explained by the independent and interacting effects of a subset of traits (Appendix S1: Table S7). The most important traits for predicting phenotype-level mortality were also the most important for predicting tree-level mortality. For example, mortality rates were lower for trees and phenotypes with greater potential to grow above the forest canopy (high H_{max}), with higher radiation-use efficiency (high ϵ), and/or with stems supporting more conducting area (high γ_X), which would allow for greater investment in height growth.

The tree- and phenotype-level mortality regressions are generally consistent with empirical studies. For example, maximum potential height of a mature tree (H_{max}) often emerges as a predictor of population- or species-level mortality (e.g., Poorter et al. 2008, Wright et al. 2010, Ruger et al. 2012); trees or phenotypes associated with high H_{max} are less likely to die during closed-canopy phases. This relationship may be expected if a tree with the potential for high H_{max} can also grow fast, allowing it to quickly position its crown above the forest canopy. However, some studies show that H_{max} is only a weak predictor of mortality for species associated with $H_{\text{max}} > 25$ m (Ruger et al. 2012), or for seedlings as seedling growth rates do not necessarily correlate with H_{max} (Wright et al. 2010). Thus, it appears that the degree to which H_{max} can serve as a predictor of mortality

may depend on species identity and the growth stage of the tree.

In addition to H_{max} , we also found that radiation-use efficiency (ϵ) was just as, or more, important for predicting mortality. This trait is related to how efficiently light is used to acquire carbon, with higher values being especially beneficial in low light. Empirical studies indicate that ϵ is related to leaf nitrogen content (Sinclair and Horie 1989, Wang et al. 1991, Martin and Jokela 2004), which in turn is related to a number of other leaf traits, including specific leaf area (SLA), leaf life span, and mass-based photosynthetic rate (Wright et al. 2004). Thus, it is also possible that the importance of ϵ could reflect the combined contribution of these other, related traits for predicting tree-, phenotype-, population-, and/or species-level mortality.

While we also found that the conducting area to sapwood area ratio (γ_X) was an important predictor of mortality under light stress, this trait is rarely measured in field studies that attempt to link mortality to functional traits. While γ_X can be measured (e.g., Hacked et al. 2001, Kaakinen et al. 2004, Lens et al. 2005, 2011), such measurements are time consuming and potentially challenging, which likely explains the reporting of limited data related to this trait. However, our simulation experiments indicate that this may be an important trait to target in mortality studies. In contrast, many empirical studies have reported relationships between wood density (ρ) and tree mortality, where lower ρ is typically related to higher mortality rates (Poorter et al. 2008, Chave et al. 2009, Wright et al. 2010). But, ρ did not emerge as a top predictor of mortality in our analyses. However, ρ in the ACGCA model describes the density of wood formed under “optimal” conditions. In reality, bulk ρ varies from year to year (Bouriaud et al. 2005, Skomarkova et al. 2006), and field-based measurements of ρ represent a composite trait that reflects anatomical features, such as γ_X and cell wall thickness. Thus, our finding that γ_X is a key predictor of mortality is consistent with the observation that field-based ρ is often predictive of mortality, but suggests that mortality may be indirectly linked to ρ via its relationship to γ_X .

Finally, in the ACGCA model, tree death occurs when the labile carbon pools have been depleted. Thus, parameters (or traits) that are the best predictors of labile carbon dynamics are expected to also be important for predicting mortality. In previous work, we conducted a sensitivity analysis to identify the traits to which changes in a tree’s relative labile carbon pool are most sensitive (Fell et al. 2018). Labile carbon pools in both young (simulation years 1–10) and mature (simulation years 41–50) trees were found to be sensitive to traits that also emerged as the best predictors of tree- and phenotype-level mortality in this study, such as H_{max} and γ_X (Fell et al. 2018). Similarly, both radial and height growth of young trees were sensitive to ϵ and R_0 , and mature trees were also sensitive to S_O (Fell et al. 2018). Thus, based on the mechanisms captured in the ACGCA model, traits influencing mortality do so either through their influence on labile carbon dynamics or radial and/or height growth.

The multi-dimensional trait space

Centroids and volumes.—Our third question asks how environmental filtering can modify the trait space. We found

that the trait spaces (hypercubes) were altered by selective mortality, supporting the concept that environmental filtering restricts the functional trait space (Van der Valk 1981, Webb et al. 2010). When comparing surviving trees to the potential population of trees, as captured by the TTS, both centroid distances and volume differences became greater as mortality increased (e.g., Fig. 4a and 4d), implying a restriction of the multidimensional trait space under light limitation. This is in agreement with a recent empirical study, using data from over 10,000 species, that found that plants have a highly restricted trait space relative to what is theoretically possible given the overall range of observed trait values (Díaz et al. 2016). Why does theory suggest that so many combinations of traits are possible relative to what is observed in the field or predicted under filtering processes? A few potential explanations include mass conservation or engineering trade-offs (Scheiter et al. 2013), competition, or natural selection (Levine 2015). Our study suggests mass conservation and engineering trade-offs are important in that a restricted trait space emerged from an individual-based model (ACGCA) subjected to only one environmental limitation (light); such trade-offs are built into this model to ensure carbon mass balance and realistic allometries (e.g., Ogle and Pacala 2009). However, this finding does not exclude competition or natural selection as potentially important since they were not explicitly assessed in this study.

Trait variation.—For those traits that were the best predictors of tree- and/or phenotype-level mortality, their distributions differed among the surviving and dead groups of trees (for H_{max} , ϵ , and γ_X , see Fig. 1b–d). The location of each univariate, marginal distribution clearly differed between the two groups (e.g., the mean or mode of H_{max} was lower for dead compared to surviving trees; Fig. 1a), but the spread or variance did not notably differ. The univariate location differences agree with the hypercube results in that the centroids (an index of location in multivariate space) significantly differed between the two groups of trees, with distances being greatest under gap scenarios leading to low stand-level mortality, but approaching zero as mortality approached 50% (Fig. 4c and Appendix S1: Fig. S2c). The similarity in spread among the univariate distributions (Fig. 1b–d) seemingly conflicts with the hypercube volumes (i.e., indices of “spread” in six dimensions). For example, as for the centroid distances, volume differences were greatest under low stand-level mortality, but disappeared as mortality rates approached 50% (Fig. 4f and Appendix S1: Fig. S2f). Overall, the trait space of dead trees was narrower (smaller volume) under low mortality conditions compared to the surviving trees, indicating that very specific combinations or ranges of traits were “selected against” under comparatively low light stress. As light stress increased, a larger proportion of trees died, thus expanding the trait space associated with the dead group of trees, while simultaneously shrinking the trait space associated with surviving trees.

The apparent inconsistency between the marginal distributions for individual traits and the hypercube characteristics may be explained by the covariance structure of the multidimensional trait space. This covariance structure

implies that traits within the trait space may be correlated, reflecting the possibility that a tree can respond to a given stressor in different ways (i.e., via different combinations of trait values). In support of this, a simulation that employed a genetic algorithm to identify the trait values—for 34 functional traits—that optimize seedling growth, survival, and fitness produced multiple, essentially infinite, combinations of “optimal” trait values that spanned up to two orders of magnitude (Marks and Lechowicz 2006). This was attributed to the concept that even in a heterogeneous environment, it is possible to have many optimal solutions, provided that some traits strongly covary with each other, potentially reflecting important trait trade-offs (Marks and Lechowicz 2006). Similar results were also found in a laboratory study of evolution in bacteria where uniform environments were found to lead to similar levels of fitness even though genetic divergence and changes in individual traits occurred over 1,000 generations (Korona 1996). Unfortunately, it would be impractical to conduct an observational experiment of this type for long-lived trees, pointing to the utility of simulation experiments.

Though we do not explicitly model competition between individuals, a recent study found that trait dissimilarity is not critical for determining local competitive effects on growth (Kunstler et al. 2016). For example, a trade-off in performance could permit the coexistence of species with diverse traits, when competition is present vs. when competition is absent, provided disturbance (such as gap formation) creates an environment with multiple successional stages (Kunstler et al. 2016). Our results support this in that they generally show wide ranges of trait values can be present in surviving individuals, even as stand-level mortality approaches 50%. This implies multiple strategies exist, allowing individuals to tolerate relatively inhospitable environments (here, low light). However, the trait space would likely become highly restricted if stand-level mortality were to continue increasing, and as it approaches 100%, we would predict that the trait space describing trees capable of tolerating increasingly lower light would become much less variable (narrower [univariate] or smaller volume [multi-variate]).

Limitations and future directions

The creation of the TTS (Fell et al. 2018) and the evaluation of filtering processes affecting the functional trait space of trees was based on simulation experiments conducted with an individual-based model of tree growth and mortality (ACGCA; Ogle and Pacala 2009). The current version of ACGCA is only driven by one environmental variable: light. Given our overarching goal to assess the TTS for North American trees and the effect of environmental stress (gap dynamics) on refining this trait space, limiting the environmental drivers to only light eased interpretation of the results. However, the simplicity of the gap dynamics simulations and the coarse physiology sub-model limit extension of our results to other filtering processes and environmental stressors. In reality, trees can experience a multitude of limitations, leading to a wide variety of trait trade-offs (Wright et al. 2004, Chave et al. 2009, Scheiter et al. 2013, Díaz et al. 2016, Kunstler et al. 2016). Even with the limitations implied by only considering one environmental variable,

meaningful changes in the trait space were identified, and the presence of realistic, multidimensional relationships between traits emerged. Including more physiological processes and drivers in the ACGCA model would allow us to explore the impacts of other stressors (e.g., drought) or interacting stressors (e.g., drought and shading) on the trait space. It is likely that the key traits predicting mortality under different stressors (e.g., drought, nutrient limitation) would likely differ from the important traits identified here that relate to mortality under light limitation.

One of our goals is to integrate the ACGCA model with more detailed physiological sub-models (e.g., photosynthesis [Farquhar et al. 1980], stomatal conductance [Ball et al. 1987, Medlyn et al. 2011], hydraulics [Sperry et al. 1998, Tuzet et al. 2003]), allowing the investigation of additional stressors and associated physiological limitations. For instance, incorporation of a sub-model for water uptake, transport, and transpiration would permit the integration of soil moisture availability, plant water relations, and photosynthesis (Sperry et al. 1998, Tuzet et al. 2003). A second goal is to integrate the ACGCA model with a forest stand model that would enable explicit representation of competition and community dynamics, such as the Perfect Plasticity Approximation (PPA; Purves et al. 2008, Strigul et al. 2008), SORTIE (Pacala et al. 1993, 1996), or the Ecosystem Demography (ED; Moorcroft et al. 2001) models, thus allowing for the evaluation of both biotic and environmental filters. There is the potential to simultaneously implement these modifications, provided the computational challenges can be overcome. This may be possible if the sub-models are chosen carefully. Some guidance could come from work on dynamic global vegetation models (DGVMs) that integrate functional traits and individual-level processes in a computationally tractable way (Scheiter et al. 2013, Fyllas et al. 2014).

CONCLUSIONS

Through a series of simulation experiments with a semi-mechanistic model of tree growth and carbon allocation, we found that non-random mortality induced by light limitation led to a refinement of the functional trait space occupied by trees. This was demonstrated through changes in the hypercube characteristics that define the multidimensional trait spaces occupied by surviving trees and dead trees compared to the theoretical trait space (TTS). Moreover, while average light level was a good predictor of stand-level mortality, tree- and phenotype-level mortality were best explained by a subset of the 32 traits in the TTS. For example, maximum height (H_{max}), radiation use efficiency (ϵ), and the conducting area to sapwood area ratio (γ_X) were consistently identified as important predictors of mortality. Given that only a few (about six) traits were strong predictors of mortality, this supports assertions that there is an upper limit to the number of traits needed to explain ecological processes such as community assembly (Laughlin 2014). Finally, many of the trait-mortality relationships that emerged from the relatively simple gap dynamics simulations were generally in agreement with empirical studies, suggesting that model-based approaches, as described here, may be helpful in understanding relationships that may not be evident or practical to investigate through empirical

approaches. Model-based approaches may also be useful for understanding how trees respond to novel environmental conditions, especially if the models include additional environmental constraints such as temperature and precipitation and their impacts on carbon balance and mortality.

ACKNOWLEDGMENTS

This work was partially supported by an NSF-Division of Biological Infrastructure grant to K. Ogle (#0850361). We thank Abraham Cadmus, Jessica Guo, Yao Liu, Drew Peltier, Kimberly Samuels-Crow, and Larissa Yocom-Kent for valuable input on the manuscript. We also thank Michael Fell's committee members for their support and feedback, including Janet Franklin, Thomas Day, Kevin Hultine, and Jarrett Barber.

LITERATURE CITED

- Ball, J., I. Woodrow, and J. Berry. 1987. A model predicting stomatal conductance and its contribution to the control of photosynthesis under different environmental conditions. Pages 221–224 in J. Biggins, editor. *Progress in photosynthesis research*. Springer, Dordrecht, The Netherlands.
- Blonder, B., C. Lamanna, C. Violle, and B. J. Enquist. 2014. The n-dimensional hypervolume. *Global Ecology and Biogeography* 23:595–609.
- Botkin, D. B., J. F. Janak, and J. R. Wallis. 1972. Some ecological consequences of a computer model of forest growth. *Journal of Ecology* 60:849–872.
- Bouriaud, O., J.-M. Leban, D. Bert, and C. Deleuze. 2005. Intra-annual variations in climate influence growth and wood density of Norway spruce. *Tree physiology* 25:651–660.
- Bugmann, H. 2001. A review of forest gap models. *Climatic Change* 51:259–305.
- Chave, J., D. Coomes, S. Jansen, S. L. Lewis, N. G. Swenson, and A. E. Zanne. 2009. Towards a worldwide wood economics spectrum. *Ecology Letters* 12:351–366.
- Clark, J. S., et al. 2010. High-dimensional coexistence based on individual variation: a synthesis of evidence. *Ecological Monographs* 80:569–608.
- Cornwell, W. K., and D. D. Ackerly. 2009. Community assembly and shifts in plant trait distributions across an environmental gradient in coastal California. *Ecological Monographs* 79:109–126.
- Devictor, V., D. Mouillot, C. Meynard, F. Jiguet, W. Thuiller, and N. Mouquet. 2010. Spatial mismatch and congruence between taxonomic, phylogenetic and functional diversity: The need for integrative conservation strategies in a changing world. *Ecology Letters* 13:1030–1040.
- Díaz, S., et al. 2016. The global spectrum of plant form and function. *Nature* 529:167–171.
- Evans, M. R., K. J. Norris, and T. G. Benton. 2011. Predictive ecology: systems approaches. *Philosophical Transactions of the Royal Society B* 367:163–169.
- Falster, D. S., and M. Westoby. 2005. Alternative height strategies among 45 dicot rain forest species from tropical Queensland, Australia. *Journal of Ecology* 93:521–535.
- Farquhar, G. D., S. Caemmerer, and J. A. Berry. 1980. A biochemical model of photosynthetic CO₂ assimilation in leaves of C₃ species. *Planta* 149:78–90.
- Fell, M., J. Barber, J. W. Lichstein, and K. Ogle. 2018. Multidimensional trait space informed by a mechanistic model of tree growth and carbon allocation. *Ecosphere* 9:e02060.
- Fyllas, N. M., et al. 2014. Analysing Amazonian forest productivity using a new individual and trait-based model (TFS v.1). *Geoscientific Model Development* 7:1251–1269.
- Gelman, A., J. B. Carlin, H. S. Stern, D. B. Dunson, A. Vehtari, and D. B. Rubin. 2014. *Bayesian data analysis*. Third edition. CRC Press, New York, New York, USA.
- Givnish, T. J. 1988. Adaptation to sun and shade. *Australian Journal of Plant Physiology* 15:63–92.
- Grömping, U. 2006. Relative importance for linear regression in R: the package relaimpo. *Journal of Statistical Software* 17:139–147.
- Hacke, U. G., J. S. Sperry, W. T. Pockman, S. D. Davis, and K. A. McCulloh. 2001. Trends in wood density and structure are linked to prevention of xylem implosion by negative pressure. *Oecologia* 126:457–461.
- Kaakinen, S., K. Kostianen, F. Ek, P. Saranpää, M. E. Kubiske, J. Sober, D. F. Karnosky, and E. Vapaavuori. 2004. Stem wood properties of *Populus tremuloides*, *Betula papyrifera* and *Acer saccharum* saplings after 3 years of treatments to elevated carbon dioxide and ozone. *Global Change Biology* 10:1513–1525.
- Kattge, J., K. Ogle, G. Bönisch, S. Díaz, S. Lavorel, J. Madin, K. Nadrowski, S. Nöllert, K. Sartor, and C. Wirth. 2011. A generic structure for plant trait databases. *Methods in Ecology and Evolution* 2:202–213.
- Korona, R. 1996. Genetic divergence and fitness convergence under uniform selection in experimental populations of bacteria. *Genetics* 143:637–664.
- Kraft, N. J. B., P. B. Adler, O. Godoy, E. C. James, S. Fuller, and J. M. Levine. 2015. Community assembly, coexistence and the environmental filtering metaphor. *Functional Ecology* 29:592–599.
- Kunstler, G., et al. 2016. Plant functional traits have globally consistent effects on competition. *Nature* 529:1–15.
- Laughlin, D. C. 2014. The intrinsic dimensionality of plant traits and its relevance to community assembly. *Journal of Ecology* 102:186–193.
- Lens, F., S. Dressler, S. Jansen, L. van Evelghem, and E. Smets. 2005. Relationships within balsaminoid Ericales: a wood anatomical approach. *American Journal of Botany* 92:941–953.
- Lens, F., J. S. Sperry, M. A. Christman, B. Choat, D. Rabaey, and S. Jansen. 2011. Testing hypotheses that link wood anatomy to cavitation resistance and hydraulic conductivity in the genus *Acer*. *New Phytologist* 190:709–723.
- Levine, J. M. 2015. A trail map for trait-based studies. *Nature* 529:163–164.
- MacArthur, R., and R. Levins. 1967. The limiting similarity, convergence, and divergence of coexisting species. *American Naturalist* 101:377–385.
- Marks, C. O., and M. J. Lechowicz. 2006. Alternative designs and the evolution of functional diversity. *American Naturalist* 167:55–66.
- Martin, T. A., and E. J. Jokela. 2004. Developmental patterns and nutrition impact radiation use efficiency components in southern pine stands. *Ecological Applications* 14:1839–1854.
- McCarthy, J. 2001. Gap dynamics of forest trees: A review with particular attention to boreal forests. *Environmental Reviews* 59: 1–59.
- McGill, B. J., B. J. Enquist, E. Weiher, and M. Westoby. 2006. Rebuilding community ecology from functional traits. *Trends in Ecology and Evolution* 21:178–185.
- McMahon, S. M., C. J. E. Metcalf, and C. W. Woodall. 2011. High-dimensional coexistence of temperate tree species: functional traits, demographic rates, life-history stages, and their physical context. *PLoS ONE* 6:e16253.
- Medlyn, B. E., R. A. Duursma, D. Eamus, D. S. Ellsworth, I. C. Prentice, C. V. M. Barton, K. Y. Crous, P. De Angelis, M. Freeman, and L. Wingate. 2011. Reconciling the optimal and empirical approaches to modelling stomatal conductance. *Global Change Biology* 17:2134–2144.
- Moorcroft, P. R., G. C. Hurtt, and S. W. Pacala. 2001. A method for scaling vegetation dynamics: the ecosystem demography model (Ed). *Ecological Monographs* 71:557–586.
- Ogle, K., and S. W. Pacala. 2009. A modeling framework for inferring tree growth and allocation from physiological, morphological and allometric traits. *Tree Physiology* 29:587–605.
- Ogle, K., J. Barber, and K. Sartor. 2013. Feedback and modularization in a Bayesian meta-analysis of tree traits affecting forest dynamics. *Bayesian Analysis* 8:133–168.
- Ogle, K., S. Pathikonda, K. Sartor, J. W. Lichstein, J. L. D. Osnas, and S. W. Pacala. 2014. A model-based meta-analysis for estimating

- species-specific wood density and identifying potential sources of variation. *Journal of Ecology* 102:194–208.
- Pacala, S. W., C. D. Canham, and J. A. Jr Silander. 1993. Forest models defined by field measurements: I. The design of a north-eastern forest simulator. *Canadian Journal of Forest Research* 23:1980–1988.
- Pacala, S. W., C. D. Canham, J. Saponara, J. A. Jr Silander, R. K. Kobe, and E. Ribbens. 1996. Forest models defined by field measurements: estimation, error analysis and dynamics. *Ecological Monographs* 66:1–43.
- Pearl, R., and L. J. Reed. 1920. On the rate of growth of the population of the United States since 1790 and its mathematical representation. *Proceedings of the National Academy of Sciences USA* 6:275–288.
- Poorter, L. 1999. Growth responses of 15 rain forest tree species to a light gradient; the relative importance of morphological and physiological traits. *Functional Ecology* 13:396–410.
- Poorter, L., and F. Bongers. 2006. Leaf traits are good predictors of plant performance across 53 rain forest species. *Ecology* 87:1733–1743.
- Poorter, L., et al. 2008. Are functional traits good predictors of demographic rates? Evidence from five neotropical forests. *Ecology* 89:1908–1920.
- Purves, D. W., J. W. Lichstein, N. Strigul, and S. W. Pacala. 2008. Predicting and understanding forest dynamics using a simple tractable model. *Proceedings of the National Academy of Sciences USA* 105:17018–17022.
- Reich, P. B. 2014. The world-wide “fast-slow” plant economics spectrum: a traits manifesto. *Journal of Ecology* 102:275–301.
- Ruger, N., C. Wirth, S. J. Wright, and R. Condit. 2012. Functional traits explain light and size response of growth rates in tropical tree species. *Ecology* 93:2626–2636.
- Runkle, J. R. 1985. Disturbance regimes in temperate forests. Pages 17–33 in S. T. A. Pickett, and P. S. White, editors. *The ecology of natural disturbance and patch dynamics*. Academic Press, London, UK.
- Runkle, J. R., and T. C. Yetter. 1987. Treefalls revisited: gap dynamics in the southern Appalachians. *Ecology* 68:417–424.
- Savage, V. M., C. T. Webb, and J. Norberg. 2007. A general multi-trait-based framework for studying the effects of biodiversity on ecosystem functioning. *Journal of Theoretical Biology* 247:213–229.
- Scheiter, S., L. Langan, and S. I. Higgins. 2013. Next-generation dynamic global vegetation models: Learning from community ecology. *New Phytologist* 198:957–969.
- Sinclair, T. R., and T. Horie. 1989. Leaf nitrogen, photosynthesis, and crop radiation use efficiency: a review. *Crop Science* 29:90.
- Skomarkova, M. V., E. A. Vaganov, M. Mund, A. Knohl, P. Linke, A. Boerner, and E. D. Schulze. 2006. Inter-annual and seasonal variability of radial growth, wood density and carbon isotope ratios in tree rings of beech (*Fagus sylvatica*) growing in Germany and Italy. *Trees* 20:571–586.
- Sperry, J. S., F. R. Adler, G. S. Campbell, and J. P. Comstock. 1998. Limitation of plant water use by rhizosphere and xylem conductance: results from a model. *Plant, Cell and Environment* 21:347–359.
- Stahl, U., J. Kattge, B. Reu, W. Voigt, and K. Ogle. 2013. Whole-plant trait spectra of North American woody plant species reflect fundamental ecological strategies. *Ecosphere* 4:128.
- Strigul, N. I. S., D. Pristinski, D. Purves, J. Dushoff, S. Pacala, D. E. P. Ristinski, D. R. E. W. P. Urves, and J. O. D. Ushoff. 2008. Scaling from trees to forests: tractable macroscopic equations for forest dynamics. *Ecological Monographs* 78:523–545.
- Stubbs, W. J., and J. B. Wilson. 2004. Evidence for limiting similarity in a sand dune community. *Journal of Ecology* 92:557–567.
- Tilman, D. 1985. The resource-ratio hypothesis of plant succession. *American Naturalist* 125:827–852.
- Tuzet, A., A. Perrier, and R. Leuning. 2003. A coupled model of stomatal conductance, photosynthesis and transpiration. *Plant, Cell and Environment* 26:1097–1116.
- Valverde, T., and J. Silvertown. 1997. Canopy closure rate and forest structure. *Ecology* 78:1555–1562.
- Van Bodegom, P. M., J. C. Douma, and L. M. Verheijen. 2014. A fully traits-based approach to modeling global vegetation distribution. *Proceedings of the National Academy of Sciences USA* 111:13733–13738.
- Van der Valk, A. G. 1981. Succession in wetlands: a Gleasonian approach. *Ecology* 62:688–696.
- Violle, C., P. B. Reich, S. W. Pacala, B. J. Enquist, and J. Kattge. 2014. The emergence and promise of functional biogeography. *Proceedings of the National Academy of Sciences USA* 111:13690–13696.
- Wang, A. Y. P., P. G. Jarvis, and C. M. A. Taylor. 1991. PAR absorption and its relation to above-ground dry matter production of Sitka spruce. *Journal of Applied Ecology* 28:547–560.
- Webb, C. T., J. A. Hoeting, G. M. Ames, M. I. Pyne, and N. LeRoy Poff. 2010. A structured and dynamic framework to advance traits-based theory and prediction in ecology. *Ecology Letters* 13:267–283.
- Weier, E., and P. Keddy. 1999. Introduction: the scope and goals of research on assembly rules. Pages 1–19 in W. Evan, and K. Paul, editors. *Ecological assembly rules: perspectives, advances, retreats*. First. Cambridge University Press, New York, New York, USA.
- Weier, E., A. van der Werf, K. Thompson, M. Roderick, E. Garnier, and O. Eriksson. 1999. Challenging Theophrastus: a common core list of plant traits for functional ecology. *Journal of Vegetation Science* 10:609–620.
- Westoby, M., and I. J. Wright. 2006. Land-plant ecology on the basis of functional traits. *Trends in Ecology & Evolution* 21:261–268.
- Woodward, F. I., and A. D. Diament. 1991. Functional approaches to predicting the ecological effects of global change. *Functional Ecology* 5:202–212.
- Wright, I. J., et al. 2004. The worldwide leaf economics spectrum. *Nature* 428:821–827.
- Wright, S. J., et al. 2010. Functional traits and the growth—mortality trade-off in tropical trees. *Ecology* 91:3664–3674.

SUPPORTING INFORMATION

Additional supporting information may be found online at: <http://onlinelibrary.wiley.com/doi/10.1002/ecm.1294/full>

DATA AVAILABILITY

Data associated with this study are available from the Dryad Digital Repository: <https://doi.org/10.5061/dryad.8bm78>.